AD-A115 910 CATHOLIC UNIV OF AMERICA WASHINGTON DC VITREOUS STATE LAB F/G 20/6
RADIATION HARDENING OF STRENGTHENED OPTICAL FIBERS AND DEVELOPM--ETC(U)
APR 82 R K MOHR, J H SIMMONS, C T MOYNIHAN F19628-79-C-0061
UNCLASSIFIED RADC-TR-82-86 NL

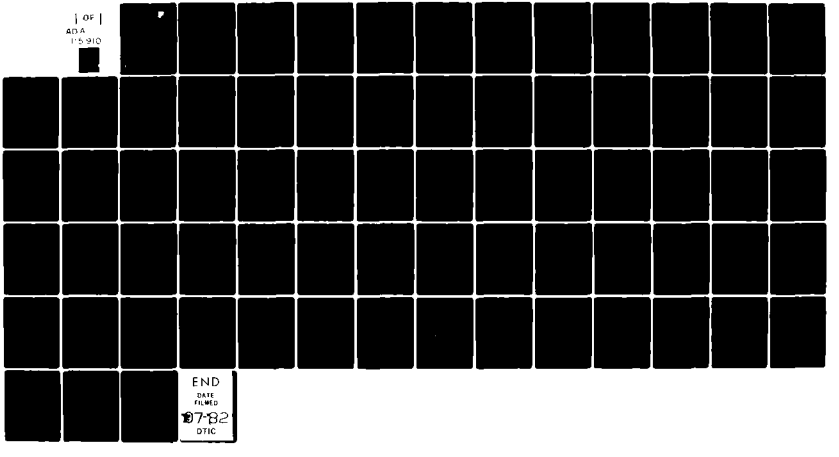

RADC-TR-82-86
Final Technical Report
April 1982

RADIATION HARDENING OF STRENGTHENED OPTICAL FIBERS AND DEVELOPMENT OF NEW FLUORIDE GLASSES

Catholic University of America

R.K. Mohr, J.H. Simmons, C.T. Moynihan, A. Barkatt, H. Hojaji,
C. Williams, M.S. Boulos, E.O. Gbogi and K.H. Chung

ROME AIR DEVELOPMENT CENTER
Air Force Systems Command
Griffiss Air Force Base, NY 13441

This report has been reviewed by the RADC Public Affairs Office (PA) and is releasable to the National Technical Information Service (NTIS). At NTIS it will be releasable to the general public, including foreign nations.

RADC-TR-82-86 has been reviewed and is approved for publication.

APPROVED: Martin G. Drexhage

MARTIN G. DREXHAGE
Project Engineer

APPROVED: Harold Roth

HAROLD ROTH
Director, Solid State Sciences Division

FOR THE COMMANDER: John P. Huss

JOHN P. HUSS
Acting Chief, Plans Office

If your address has changed or if you wish to be removed from the RADC mailing list, or if the addressee is no longer employed by your organization, please notify RADC (ESM) Hanscom AFB MA 01731. This will assist us in maintaining a current mailing list.

Do not return copies of this report unless contractual obligations or notices on a specific document requires that it be returned.

UNCLASSIFIED

SECURITY CLASSIFICATION OF THIS PAGE (When Data Entered)

REPORT DOCUMENTATION PAGE	READ INSTRUCTIONS BEFORE COMPLETING FORM
1. REPORT NUMBER: RADC-TR-82-86	2. GOVT ACCESSION NO.	3. RECIPIENT'S CATALOG NUMBER
4. TITLE (and Subtitle): RADIATION HARDENING OF STRENGTHENED OPTICAL FIBERS AND DEVELOPMENT OF NEW FLOURIDE GLASSES	5. TYPE OF REPORT & PERIOD COVERED: Final Technical Report 1 Feb 79 - 30 Sep 80
	6. PERFORMING ORG. REPORT NUMBER: N/A
7. AUTHOR(s): R. K. Mohr, A. Barkatt, M. S. Boulos, J.H. Simmons, H. Hojaji, E. O. Gbogi, C.T. Moynihan, C. Williams, K. H. Chung	8. CONTRACT OR GRANT NUMBER(s): F19628-79-C-0061
9. PERFORMING ORGANIZATION NAME AND ADDRESS: Catholic University of America, Vitreous State Laboratory, Wash DC 20064	10. PROGRAM ELEMENT, PROJECT, TASK AREA & WORK UNIT NUMBERS: 62702F, 46001737
11. CONTROLLING OFFICE NAME AND ADDRESS: Deputy for Electronic Technology (RADC/ESM), Hanscom AFB MA 01731	12. REPORT DATE: April 1982
	13. NUMBER OF PAGES: 69
14. MONITORING AGENCY NAME & ADDRESS (if different from Controlling Office): Same	15. SECURITY CLASS. (of this report): UNCLASSIFIED
	15a. DECLASSIFICATION/DOWNGRADING SCHEDULE: N/A

16. DISTRIBUTION STATEMENT (of this Report)

Approved for public release; distribution unlimited.

17. DISTRIBUTION STATEMENT (of the abstract entered in Block 20, if different from Report)

Same

18. SUPPLEMENTARY NOTES

RADC Project Engineer: Martin Drexhage (ESM)

19. KEY WORDS (Continue on reverse side if necessary and identify by block number)

Fiber optics
Radiation hardening
Fluoride glasses

20. ABSTRACT (Continue on reverse side if necessary and identify by block number)

Two independent studies were conducted under this contract:
1. Radiation hardening of compressively strengthened optical fibers;
2. Development of new flouride glasses. In the first study two preform fabrication processes based on phase separable, leachable alkali borosilicate glasses were evaluated for producing radiation hardened fibers. The first process, known as partial leaching, was found to yield low numerical aperture fibers with moderately high attenuation. Ultra-

DD FORM 1 JAN 73 1473 EDITION OF 1 NOV 65 IS OBSOLETE

UNCLASSIFIED

SECURITY CLASSIFICATION OF THIS PAGE (When Data Entered)

clean glass melting facilities and extensive composition studies would be required to correct these faults. This was beyond the resources of the contract. The second process, known as molecular stuffing, was used to produce alkali-modified high silica glasses doped with cerium oxide as a radiation hardening agent. Radiation damage kinetic tests were run on these glasses by irradiating the samples with 4-40 ns pulses of 15 MeV electrons and observing the absorption spectra for the time range 10^{-7}s to 10^{-1}s following the electron pulses. The results of these tests show that cerium is not effective, within the time range studies, in suppressing the radiation induced absorption for the high silica glasses tested. In the second study, under this contract, glasses in the HfF_4-BaF_2-LaF_3 family were studied. The effects on glass forming of additions including PbF_2, CsF, GdF_3 and AlF_3 glass was studied. Glass transition and crystallization temperatures were determined for these glasses. Finally the effects of -OH impurities were measured and a method was found for eliminating -OH from the bulk region of the glass samples.

TABLE OF CONTENTS

A

I. Summary

There were two major objectives of this contract:

1. To develop and study strengthened radiation hardened communications grade optical fibers.
2. The development and study of new fluoride glasses.

The first of these objectives was concerned with optical waveguides which transmit in the visible and near infrared, while the second objective was concerned with new glasses transmitting from the visible through the mid IR and which could lead to new optical waveguide glasses. The approaches to these two objectives are very different and thus the contract was divided into two independent projects.

The first project consisted primarily of evaluating and improving processes developed under past research grants and determining their applicability to strengthening and radiation hardening. The second project consisted of developing new processes and materials.

A. Strengthened Radiation Hardened Optical Fibers

Two approaches to the first project were undertaken. The first was a study of the application of a "partial leaching" process, developed for strengthening glass, to the development of a strong radiation hardened optical fiber waveguide. The partial leaching process consists of the following stages:

1. Melting phase-separable, alkali borosilicate glasses and drawing them into rod preforms 0.6 - 1.0 cm in diameter by 1 meter long.

2. Heat-treating these rods to induce a liquid-liquid phase separation throughout the glass in order to form a high silica phase and a high alkali borate phase.
3. Leaching out the alkali borate phase within a thin surface layer of the glass rod, thus forming a porous high silica cladding region.
4. Sintering the porous cladding region to form a glass rod with a step index profile having a high index alkali borosilicate core and a low index, high silica clad. During cooling the difference in expansion coefficient between the core and clad induces a high compressive stress on the rod surface which acts to strengthen the glass. Prestressing values of greater than 30,000 psi have been obtained by this process.
5. Drawing the rod preform into an optical fiber.
6. In this process radiation hardening might be accomplished by adding hardening agents to the base glass during melting and or to the porous clad region after leaching.

The research conducted under this first approach was to evaluate this process for optical fiber use. Since pre-stressing and strengthening had already been demonstrated, the initial concern was that the core, consisting of a phase separable borosilicate glass would scatter light at an unacceptable level. Tests were conducted of scattering levels in both the fabricated partially leached preforms and the fibers. The tests consisted of Rayleigh scattering measurements made relative to scattering in fused silica of optical fiber quality. The results showed

that partially leached fibers, despite a small residual microstructure, exhibit low light scattering (less than 2-3 time fused silica) and therefore could be used for optical fibers.

The core of the fibers is formed by conventional melting procedures, therefore, extreme precautions are necessary to avoid contamination by transition metal impurities and a resulting high absorption. This could not be achieved within the scope of the contract, therefore, all fibers made by this method had very high absorption losses. It is anticipated that melting techniques similar to those used for fibers made by the double crucible process would yield low loss fibers.

A second problem with this approach was indicated by the results of refractive index measurements on the core and clad regions which showed a small difference in refraction index, n, leading to numerical apertures of less than 0.2 ($n_{core} \simeq 1.47$, $n_{clad} \simeq 1.46$). To increase the numerical aperture to more useful levels would require the use of a base glass very different from the alkali borosilicate glasses previously studied by us for phase separation and leaching. The studies required to develop new base glass compositions were also beyond the scope of this contract. It was thus concluded that this approach would not lead to communication grade fibers without a large additional research effort.

The second approach to the first project was to study radiation hardening in molecular stuffed fibers doped with cerium oxide. The molecular stuffing process is being used commercially to produce fibers with less than 10 dB/km

attenuation. The molecular stuffing process consists of the following stages:

1. Melting phase separable, alkali borosilicate glasses and drawing them into rod preforms 0.6 - 1.0cm in diameter by 1m long.
2. Heat-treating these rods to induce a liquid-liquid phase separation throughout the glass in order to form a high silica phase and a high alkali borate phase.
3. Leaching out the alkali borate phase throughout the rods and carefully washing the remaining porous skeleton. The majority of transition metal impurities are removed with the alkali borate phase and thus a high purity skeleton is obtained.
4. Diffusing cesium nitrate or other index modifiers and cerium nitrate salts into the porous rods to form the core region.
5. Drying and sintering the glass to form a core-clad preform composed of a high index core containing an index modifier such as Cs_2O and a low index, high silica clad glass. CeO_2 was deposited in both core and cladding regions to act as a radiation hardening agent.

The major efforts in this approach were the preparation of samples and the determination of the role that CeO_2 would play in the response of fibers to radiation damage, especially in the presence of non-negligible quantities of Fe and Cu impurities. Rod preforms containing CeO_2 were formed with a great initial difficulty due to breakage of the porous glass skeletons. After

this problem was solved, irradiation tests were conducted on cerium doped glasses which indicated that hole centers associated with SiO_2 were very stable in these glasses and that they could not be quenched by cerium. One would expect to see similar results in other high silica glasses which may explain the failure of cerium oxide as a hardening agent in these glasses.

B. Flouride Glasses

The objective of this part of the contract was to study the glass forming regions of glasses based on either ZrF_4 or HfF_4 and to improve the optical quality of these glasses. Glasses in these families have been shown to have excellent potential as materials for optical components operating in the mid-IR (2-5 μm).

As part of this study it was desired to improve the glass forming characteristics of the glasses by increasing the difference between the crystalization temperature, Tx, and glass transition temperature, Tg. By increasing this temperature difference it is found that the tendency to crystalize is suppressed. The result is an ability to form larger better quality glass forms.

The effects of composition on glass forming were examined by making a systematic melting study of the system HfF_4-BaF_3-LaF_3 in the range 55-65% HfF_4, 10-40% BaF_2, and 3-10% LaF_3 by mole percent. The effects of other additives including PbF_2, CsF, GdF_3 and AlF_3 were also studied for this system. Finally the glass 62% ZrF_4 - 33% BaF_2 - 5% LaF_3 was studied. The values of Tg and Tx were determined for these glasses using a scanning calorimeter.

In addition to the evaluation of glasses produced at Catholic University a number of glasses from the HfF_4-BaF_2-LaF_3 and ZrF_4-BaF_2-LaF_3 families produced at RADC Hanscom AFB were examined. Values of Tx and Tg were determined for these glasses.

To improve the optical quality of these glasses requires the elimination of impurities in the glasses. One of the undesireable impurities which results in excess attenuation is -OH. A study was conducted to determine whether the -OH was in the bulk of the glass or merely in a surface layer. It was found that melting in a CCl_4 atmosphere was helpful in eliminating bulk -OH and that any surface -OH formed appears to be stable over time indicating a very small rate of surface attack by atmospheric H_2O.

The results of this work on flouride glasses are incouraging and we believe that continued work in this area is justified.

II. Partial Leaching Study

A. Introduction

Partial leaching is a process for making compressively strengthened glass articles that was developed at Catholic University[1]. In that research, strengthened rods were obtained having a high silica clad and an alkali borosilicate core. It was known that the clad had a lower index than the core and thus it was expected that fibers drawn from such rods would act as optical waveguides. Since the core was phase separated it was

thought that scattering losses would be relatively high. By minor changes in composition and or fiber drawing conditions it was hoped that phase separation and thus light scattering could be suppressed to an acceptable level.

It was further recognized that low optical losses could only be obtained by ultra clean melting. Equipment for skull melting was available at RADC and a modest cooperative effort to produce pure base glasses at RADC was envisioned. The possibility of high purity conventional melting at Catholic University was also to be examined as well as the purchase of high purity glasses from commerical sources if possible.

If the waveguide properties of partial leached fibers appeared promising, a program of incorporating radiation hardening dopants in the glasses was to be undertaken. These were to be added to the base glass and or to the porous clad prior to sintering.

B. Processing

The method used to produce partially leached preforms was basically that developed by Martin Drexhage during his Ph.D research[2]. This process was optimized by him to process base glass with a composition 57.8% SiO_2, 35% B_2O_3, 1.9% Na_2O, and 5.3% K_2O. Other compositions in that family were studied having the following component ranges: SiO_2 (55-56), B_2O_3 (29-37), total alkali (4-8) in mole %. Na_2O/K_2O ratios ranged from 1.6 to 0.5. The majority of the work done in this contract was with a base glass melted in our laboratories or obtained from American Cystoscope Makers, Inc. and Pilkington Brothers with a

nominal composition of 59% SiO_2, 33.8% B_2O_3, 3.6% Na_2O and 3.6% K_2O. Modifications to Brexhage's procedure were made to reduce breakage during processing for this composition. The procedure used is given below:

Partial Leaching Process

1. Heat treatment at 515°C for 120 hours and furnance-anneal.
2. Etching in 3% HF (vol. %) for 5 minutes.
3. Leaching to the clad thickenss to radius ratio of about 0.25 in 3N HCl.
4. Water wash for about 24 hours, providing at least one change after 2 hours wash.
5. Vacuum drying for 24 hours (4 hours at room temperature and 20 hours at 75°C).
6. Temperature jump to 680°C.
7. Collapsing under reduced oxygen pressure (~ 200 mm Hg) with a heating rate of 50°C / hour to 850°C.
8. Cooling to room temperature in air.

Since there is no purification, except of the clad, inherent in this process (in contrast with the molecular stuffing process to be discussed in section III) if low optical attenuation is to be achieved ultra clean melting techniques must be used to produce the base glass. Ultra clean melting and subsequent low optical attenuation has been achieved in several research laboratories so it was expected that if partial leaching showed promise as a preform making process low losses could be achieved.

One possible technique for clean melting is known as skull melting. In this method the glass is melted by RF heating within a cooled crucible. The inner surface of the crucible becomes coated with a skin of the glass being melted so crucible contamination is prevented. This method was attempted at RADC. The alkali content of the base glass was too low to provide adequate coupling to the RF field and no heating was observed. Before any other methods of clean melting could be attempted the decision to discontinue the effort in partial leaching had been reached.

C. Property Measurements

To make an evaluation of the applicability of the partial leaching process in achieving the contract goals a number of properties were evaluated as discussed below:

1. Thermomechanical Properties

The strengthening obtained in the partial leaching process is controlled by the differential contraction between the core and clad when the fiber is cooled after drawing. The expansion coefficient α, glass transition Tg and softening temperatures Ts of the core and clad glass were measured.

Table I

	Core	Clad
α (below Tg)	65×10^{-7}/°C	8×10^{-7}/°C
α (above Tg)	280×10^{-7}/°C	
T_g	455±5°C	820°C
T_s	600°C	

Since the clad solidifies at 820°C, while the core is still liquid, the clad will be placed in compression by the relatively larger contraction of the liquid core. Further compression of the clad is obtained below the Tg of the core since its sub Tg expansion coefficient is still much larger than that of the clad. Using a simple model developed by Krohn and Cooper[3] one can predict the magnitude of the surface compression with the above data, the clad and core thicknesses, and the elastic moduli. Drexhage[2] has shown that these estimates agree well with the clad compression observed photoelastically and with improved strength as measured in modulus of rupture tests.

Measurements of the clad compression in typical partially leached preforms made during this contract ranged from 25 ksi to 35 ksi.

2. Optical Properties

a) Light Scattering Measurements

Brillouin scattering experiments were performed on two partially leached (PL) fibers supplied to us by RADC. The measurement was needed to determine a baseline for scattering losses in partially leached fibers. One of the tasks of this contract was to determine to what extent the scattering losses can be controlled by composition changes in the base glass and drawing conditions.

The fibers supplied to us were from a batch having a nominal composition of 57.8% SiO_2, 35% B_2O_3, 1.9% Na_2O and 5.3% K_2O. The fibers were furnace drawn in a graphite furnace. One fiber was supplied coated and the other uncoated.

The Landau Placzek ratios of the two fibers were 51 for the uncoated fiber and 59 for the coated fiber. This LP ratio is about 2.5 times that for fused silica so the Rayleigh scattering of such fibers would be less than 10 db/km at .8μm. This is an acceptable level for moderate loss fibers.

The Brillouin shifts were also determined for the core glass of the fiber. They were 11.9 GHz for the transverse and 20.3 GHz for the longitudinal sound waves.

b) Total Attenuation Measurements

The attenuation of fiber drawn from partially leached preforms was measured at the Vitreous State Laboratory and at RADC/ESM, Hanscomb, with similar results. The minimum attenuation was greater than 1000 dB/km, as shown in Figure 1. The iron and copper content of the batch glass was measured by colorimetric analysis to be 1 ppm or less.

The attenuation of the core glass alone was determined by making transmission measurements on several bare fibers drawn from batch glass. The attenuation is shown for two such fibers in Figure 1. The peak at 0.83μm is not understood and may be an artifact. The batch glass attenuation is nearly the same as that of the partially leached fibers but slightly worse. Since the purified clad in the partially leached fibers carries some of the transmitted energy, this may explain its slightly better performance. In both cases, however, the attenuation is high.

We show for comparison a curve (curve B in Figure 1) of batch glass produced at the Vitreous State Laboratory at a time when the melt furnace was new and relatively clean. Even in

Figure 1. Optical attenuation of several batch glass fibers A, B; of a partially leached fiber C; and a molecular stuffed fiber D.

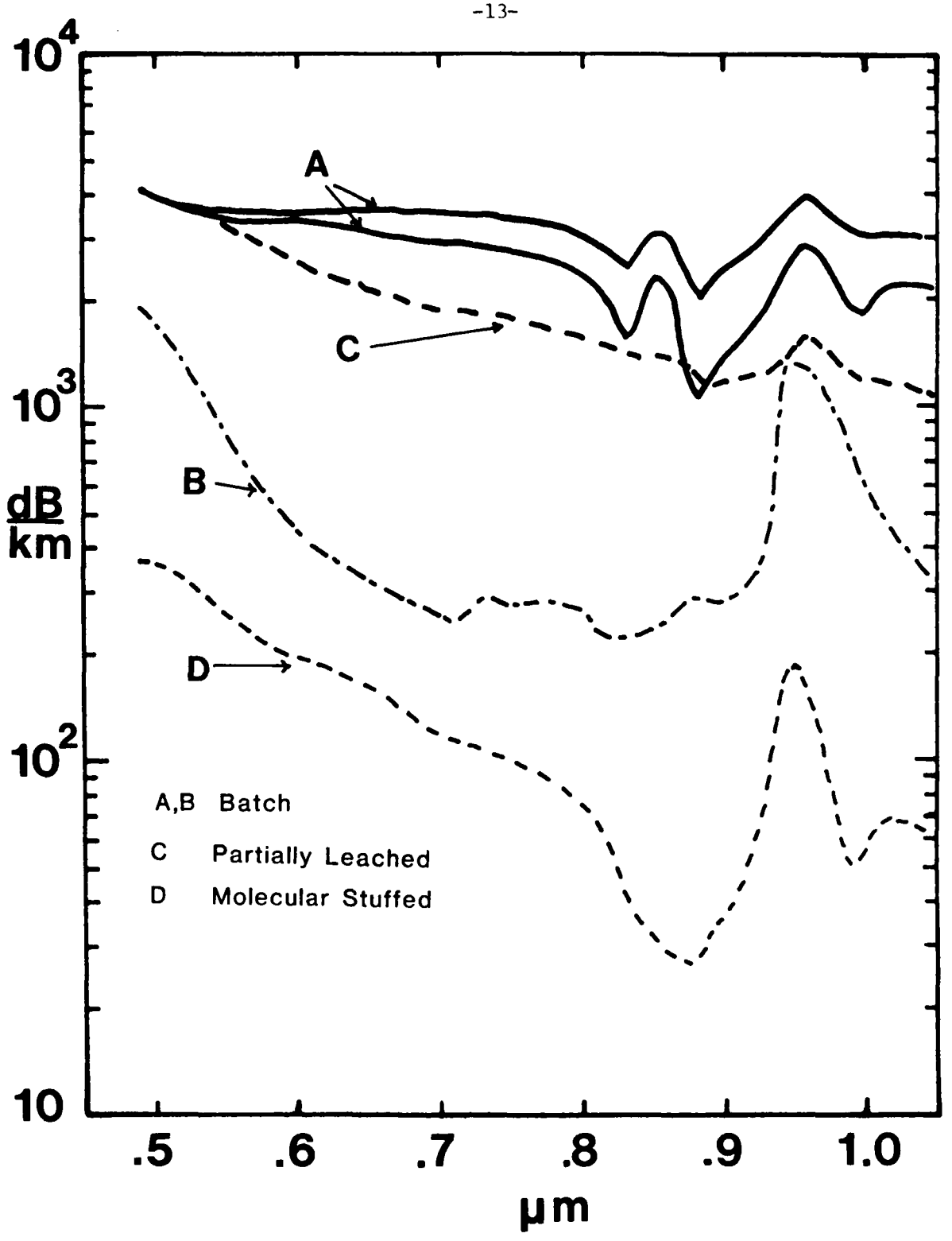
10^4
10^3
10^2
10
dB/km
A
B
C
D
A,B Batch
C Partially Leached
D Molecular Stuffed
.5
.6
.7
.8
.9
1.0
μm

this case, however, the losses are too high for useful fibers and for radiation damage studies.

To obtain lower losses would require building a melt facility in a clean room environment. This was judged to be outside the scope of the contract.

c) Refractive Index Measurements

The scattering and attenuation data on the partially leached fibers indicated that one should expect to obtain moderate loss fibers from this process. To be practical, moderate loss fibers should have a high numerical aperature. Measurement of the refractive index of the core and clad of partially leached preforms indicated refractive indices of 1.47 and 1.46 respectively. This would give a numerical aperature of less than 0.2 which is less than is desired for moderate loss multimode fibers.

To increase the refractive index of the core would require the use of a base glass with a much different composition than those previously studies by us. An extensive phase diagram study was beyond the resources available under this contract.

D. Conclusions

The major conclusion to be reached from our evaluation of the partial leaching process is that in its present state of development it does not satisfy the goals of this contract. Although no fundamental obstacles were incountered, a major effort would be required to yield very high quality fibers. No particular advantage over other competing processes was

discovered that would justify that effort at the present time. The major problems of the process are the requirement for ultra clean melting, the low numerical apertures produced using presently studied compositions and the yet unknown radiation damage characteristics.

III. Molecular Stuffing

A. Introduction

The molecular stuffing process[4,5] is a multistep process which can be used to produce high silica preforms for fiber optics production. It is an interesting process because it is suitable for batch production, it can be used to give compressively strengthened fibers and it offers the possibility of dopant combinations not easily obtained by traditional glass melting or by the various vapor phase oxidation techniques. It has the disadvantage as a multistep process of being complicated. Not all of the steps of the process are fully understood as they involve complex glass and solution chemistry and thus many of the steps have been discovered empirically. Each new dopant combination requires modifications of some of the steps and time consuming experiments to discover procedure variations which yield successful samples. The steps of the process are briefly:

1. glass melting
2. heat treatment
3. leaching

4. dopant deposition

5. dopant profiling

6. drying

7. sintering

Following the leaching step one has a purified high silica skeleton. Doping is accomplished by diffusing soluble salts into the pores and precipitating them in situ. Previous work under contract F19628-77-C-0084 had led to procedures for obtaining strengthened step index and parabolic index profiles using multiple dopants. It was planned to use these techniques to produce glasses doped with Cs and or strontium as index modifier, with cerium as a radiation hardening agent, and with Fe and Cu to act as indicators of radiation damage and healing effects. Experiments in radiation damage kinetics were conducted with such glasses at Argonne National Laboratories.

B. Sample Preparation

1. Glass Melting

Glass is melted at 1450° C from high purity industrial grade SiO_2, H_3BO_3, Na_2CO_3 and K_2CO_3. These materials typically have less than 1ppm transition metal impurities. The glass is formed into 0.7 to 1 cm by 1 meter rods by drawing from the melt.

2. Heat Treatment

The glass rods are heat treated for $1\frac{1}{2}$ to three hours at 550°C to cause phase separation. The phases have a totally interconnected structure.

3. Leaching

The rods are given a surface cleaning with 5% HF for one minute. The alkali borate phase is dissolved by placing the rods in 3N HCl at 95°C for 24 hours. The remaining porous high silica skeleton is washed in de-ionized water for 24 hours to remove the acid, any remaining leaching products and some of the silica gel from the pores. The resultant skeleton is a high purity 96% silica structure having interconnected pores approximately 100A in dimension.

4. Dopant Deposition

The porous rod is soaked in the stuffing solution containing the desired dopants (solutions used are given in Table II) for 4 hours at 105°C. After this time the dopant solution is uniformly distributed in the porous rod.

5. Dopant Profiling

The stuffed rod is placed in the appropriate unstuffing solution (which is the same as the stuffing solution less the $CsNO_3$). The unstuffing solution is at 4°C which causes the dopants to precipitate in the pores. Since the unstuffing solution contains all of the dopants except cesium nitrate the cesium nitrate is dissolved from a layer at the rod surface. The cesium free layer leads to a low index optical clad in the final preform. Unstuffing is allowed to proceed until the desired clad thickness is obtained. The rod is then soaked for four hours in a 4°C methanol solution containing all of the dopants except cesium nitrate. This is followed by placing the rod in ether at 4°C for twenty minutes. This step insures

complete precipitation of all the remaining dopants. This process gives a step index profile due to the cesium distribution. The remaining dopants are uniformly distributed throughout the rod.

6. Drying and Sintering

The solvent in the preforms is evaporated under vacuum at 4°C. The temperature is then slowly raised (15°C/hr) from room temperature to 625°C. Depending on whether reducing or oxidizing conditions are desired foaming gas (95% N_2, 5%H_2)or O_2 is flowed over the samples for 3 hours at 625°C. The temperature is then ramped to 900°C at 50°C/hr to sinter the rods. The rods are then air quenched to room temperature.

C. Spectral and Radiation Kinetics Studies

Samples for spectroscopic analysis were prepared from rods made according to the list in Table II. A specturm of each, from 2600 nm to 190 nm was run on a Spectrophotometer. The samples were then taken to Argonne National Laboritories for radiation tests as described below.

TABLE II

	Dopant (Nitrate)	Stuffing Solution*	Redox Condition	Dopant State
1)	None	-	0	-
2)	Cs	60% by weight $CsNO_3$ in H_2O	0	-
3)	Fe Cs	0.5M $Fe(NO_3)_3$ in H_2O	0	Fe^{+3}
4)	Ce Cs	0.5M $Ce(NO_3)_3$ in H_2O	0	Ce^{+4}
5)	Fe Ce Cs	0.5M $Fe(NO_3)_3$ 0.1M $Ce(NO_3)_3$ in H_2O	0	Fe^{+3}, Ce^{+4}
6)	None		R	-
7)	Cs	60% by weight $CsNO_3$ in H_2O	R	-
8)	Fe Cs	0.5M $Fe(NO_3)_3$ in H_2O	R	Fe^{+2}
9)	Ce Cs	0.5M $Ce(NO_3)_3$ in H_2O	R	Ce^{+3}
10)	Fe Ce Cs	0.1M $Fe(NO_3)_3$ 0.5M $Ce(NO_3)_3$ in H_2O	R	Fe^{+2}, Ce^{+3}

* The Stuffing Solutions all contained 60% $CsNO_3$ by weight

1. Introduction

A major source of radiation-induced attenuation of optical transmission in fiber-optic materials is the cleavage of neutral bonded units in the matrix to form sites which are electron-deficient and sites which have excess electrons. When an electron excess is created at, or in the close vicinity of, an element of the matrix which contains an Fe^{3+} impurity it tends to undergo stabilization through conversion of Fe^{3+} to Fe^{2+}. The latter species has a strong (approximately 4 $dB \cdot km^{-1} \cdot ppb^{-1}$) absorption band in the 800-1100 nm region, which is of great interest in optical fiber communications. Another contribution to the radiation-induced loss originates in absorption bands due to electron-excess and electron-deficiency centers which have not been affected by impurities. These bands are usually very broad, strongly dependent on the composition of the matrix, and although their peaks lie at shorter wavelengths they tail into the near-IR region[6-9].

A method which has been found effective in controlling radiation-induced transmission loss in the case of optical glass[10] as well as in the case of fibers[11] is the introduction of cerium. Cerium can be present in glass in two forms, as Ce^{3+} or as Ce^{4+}. The beneficial effect of Ce^{3+} is probably due to its ability to undergo oxidation by the strongly oxidizing electron-deficiency centers, (h^+), while being converted to Ce^{4+}, which has an absorption peak between 250-320 nm, depending on the composition of the medium[12]. Conversely, the presence of Ce^{4+} results in the elimination of electron-excess enters (e^-)

and the formation of Ce^{3+}, which has an absorption maximum around 230-250 nm. In both cases UV bands are formed, replacing absorption bands in the visible and near-IR regions which are detrimental in optical fiber communications. However, the presence of Ce^{4+} may have a second role which is probably not less important than the elimination of e^-, since Ce^{4+} can react with radiation-produced Fe^{2+} and oxidize it back to Fe^{3+} ($Ce^{4+} + Fe^{2+} \rightarrow Ce^{3+} + Fe^{3+}$). Both Ce^{3+} and Fe^{3+} have very low absorptivities in the near-IR region.

2. Experimental Results

The experiments carried out consisted of preparation and irradiation of high-silica glasses doped with iron and cerium. Two series of high-silica samples were prepared. In both cases molecular doping techniques were used to introduce iron and/or cerium into a porous high-silica matrix, produced through phase separation, acid leaching and washing of an alkali borosilicate glass. The doping was carried out in the presence of a large excess of cesium (introduced as $CsNO_3$) to facilitate the incorporation of Fe and/or Ce nitrates into the porous glass through thermal precipitation of $CsNO_3$ during the doping stage. This stage was followed by washing, drying, thermal decomposition of the nitrates to oxides, and consolidation of the porous structure into solid glass around 900°C, and rapid quenching in air. The resulting introduction of about 13 wt.% Cs_2O into the glass structure serves to make the Fe and Ce oxides miscible with silica, which is the major constituent of the glass. The only other components are B_2O_3 (about 4%) and Na_2O and K_2O (about 0.04% each).

The oxidation state of the dopants is determined primarily by the composition of the atmosphere under which the glass is consolidated. The first series of samples which were used in the present studies were prepared under oxygen, ensuring the presence of the dopants in their higher oxidation state. The samples included a glass doped with Ce, predominantly in the Ce^{4+} state, a glass doped with 0.5 M Fe, predominantly in the Fe^{3+} state, and a glass containing 0.5 M Fe^{3+} and 0.1 M Ce^{4+}. Each of these glasses contained 13% Cs_2O. The last sample was intended for the study of a possible reaction between radiation-produced Fe^{2+} and Ce^{4+}, while the others were intended to study the scavenging of e^- by Fe^{3+} and Ce^{4+} individually, and to serve as blank tests which would permit the isolation and identification of a Fe^{2+} - Ce^{4+} recombination process in the composite sample.

A second series of samples were prepared in a reducing environment consisting of foaming gas (5% H_2 + 95% N_2). In analogy with the first series, these samples, all of them containing 13% Cs_2O, included glasses doped with 0.5 M Ce^{3+}, 0.5 M Fe^{2+} and 0.5 M Ce^{3+} + 0.1 M Fe^{2+}, respectively. Again, it was hoped that the single-dopant samples would make it possible to detect the formation of Fe^{3+} and Ce^{4+} as a result of h^+ scavenging, and in the case of the composite sample it would be possible to monitor the reaction between Fe^{2+} and Ce^{4+}.

It should be noted that in order to make the study of a possible recombination process as direct and uncomplicated as possible, we have used a five-fold excess of Fe^{3+} over Ce^{4+} in

the combined sample of the oxidized series, so that initially the bulk of the reactive reducing radicals are trapped by Fe^{3+} to form Fe^{2+}, which later might react with Ce^{4+} to form Ce^{3+} and Fe^{3+}. The direct formation of Ce^{3+} due to competition between Ce^{4+} and Fe^{3+} with respect to reaction with the transient electron-excess radicals is minimized in this case because of the use of a glass doped with a small concentration of Ce^{4+} relative to Fe^{3+}. For an analogous reason we have used in the case of the reduced series a combined sample containing a five-fold excess of Ce^{3+} over Fe^{2+} so as to direct most of the transient hole trapping process towards the oxidation of Ce^{3+} to Ce^{4+}, which might subsequently react with Fe^{2+}, and to minimize the direct formation of Fe^{2+}.

Spectrophotometric observations on the samples showed that the iron was present to an extent of >99% as Fe^{3+} in the samples consolidated under oxygen and to the same extent as Fe^{2+} in the samples prepared under foaming gas.

The positions and intensities of the major absorption bands associated with Fe^{3+} and Fe^{2+} in high-silica glasses as established by observations on glasses prepared under oxygen and under foaming gas, respectively, are shown in Table III. The identification of cerium species was more difficult since the absorption bands of Ce^{4+} and Ce^{3+} lie in the UV region, where interference due to scattering is most serious. In the present study, measurements on Ce-containing glasses showed a significant amount of scattering, particularly in the case of oxidized samples, due to some residual microscopic phase separation. In

TABLE III

Absorption Spectra of Oxidized and Reduced Iron in High-Silica Glasses

Dopant	Feature[a]	λ nm	Absorptivity $M^{-1}cm^{-1}$	Absorptivity $dBkm^{-1}ppb^{-1}$
Fe(III)	sh	470	2.8	0.01
	s	437	6.4	0.25
	s	413	7.4	0.29
	s	375	25	0.99
	ae	301	628	24.7
Fe(II)	sh	950	91	3.6
	s	115	115	4.5
	ae	280	<800	<30

[a] sh--shoulder; s--strong peak; ae--uv absorption edge

addition, the surface finish was not optically clear. For these reasons, combined with the fact that absorption bands due to Ce^{3+} and Ce^{4+} in glasses both lie in the 230-330nm region and are both subject to strong environmental effects[12], no positive identifications of Ce^{3+} and Ce^{4+} were made in the present study. The spectroscopic data reported for these by A. Paul et. al.[12] in Na_2O - B_2O_3 glasses and by other investigators indicate that above 350nm the absorption of both Ce species is less than $2dB \cdot km^{-1} \cdot PPb^{-1}$, and while "the intensity of Ce^{3+} [as well as of Ce^{4+}] also changes with glass composition, in all the glasses the molar extinction coefficient of Ce^{4+} is 5 to 10 times stronger than that of Ce^{3+}."[12]

Finaliy, the absorption bands of radiation-produced electron-deficiency (h^+) and electron-excess (e^-) centers in alkali silicate glasses, based on studies by Stroud[6-8] and by Bishay[9] (see above), indicate that the h^+ centers are responsible for the bulk of the radiation-induced absorption in the visible region while the e^- centers have a major contribution to the UV absorption bands.

The spectroscopic features presented in Table III served as the basis for the selection of wavelength regions where transient and permanent radiation effects were monitored. The irradiation source was the Argonne National Laboratory linear electron accelerator. 15 MeV, 4 - 40ns pulses were used and the intensity of the radiation-induced absorption was followed as a function of time. Using a Faraday cup integrator, all the radiation-induced absorptions were nomalized to correspond to a

standard pulse intensity corresponding to a 10 ns pulse of approximatey 5×10^6 eV/g. (Irradiations with pulses ranging from 4 to 40ns on the same sample show the integration to be valid within 5% over the entire range.) The samples, which were rods with a diameter of (0.65±0.05)cm, were placed perpendicular to the electron beam and a 1-cm long section was exposed to irradiation. The analyzing light passed along the long axis of the rod. All the measurements were carried out at 23°C.

The results of the measurements are presented in Table IV, where the intensity of the radiation-induced absorption at various wavelengths is given (for the time range of 10^{-7} s to 10^{-1} s following the electron pulse) in absorbance units $\log_{10}(I_o/I)$, (where I_o is the intensity of the light passing through the sample before the pulse and I is the corresponding intensity measured at a certain time following the pulse).

The results obtained with 0.5 M Ce^{3+} show the presence of two radiation-produced absorption bands, one of which peaks at low wavelengths (<368nm) while the other peaks at high wavelengths (>820nm). The two bands cannot be associated with the same center, since the low-wavelength band decays only by 40% between 10^{-7} s and 10^{-1} s after the pulse while the high-wavelength band decreases by a factor of 9. It is likely that the low-wavelength band is associated with the formation of Ce^{4+} since the maximum occurs below 368 nm, and since Ce^{4+} can be expeced to be relatively stable. The high-wavelength band can be considered to be due either to stabilized (solvated) h^+, or to stabilized e^-. However, the observations that even at

TABLE IV

Radiation-Produced Absorption in High-Silica Glasses

Sample Composition	Wavelength nm	Normalized Absorbance Following Pulse 10^{-7}s	10^{-6}s	10^{-5}s	10^{-4}s	10^{-3}s	10^{-2}s	10^{-1}s
A. Oxidized Samples								
0.5M Ce^{4+}	620	0.102	0.088	0.066	0.040	0.020	0.011	0.006
	820	0.148	0.132	0.101	0.063	0.026	0.012	0.000
0.5M Fe^{3+}	620	0.059	0.054	0.050	0.042	0.041	0.036	0.033
	720				0.028	0.026	0.022	0.018
	820	0.025	0.024	0.021	0.019	0.017	0.016	0.012
0.1M Ce^{4+} + 0.5M Fe^{3+}	620	0.066	0.064	0.061	0.056	0.051	0.045	0.042
	820	0.025	0.024	0.024	0.020	0.020	0.019	0.016
	880				0.025	0.020	0.018	0.016
B. Reduced Samples								
0.5M Ce^{3+}	368	0.359	0.329	0.299	0.235	0.201		
	392.5	0.299	0.270	0.236	0.187	0.158		
	440	0.166	0.154	0.126	0.067	0.061		
	555	0.081	0.069	0.054	0.044	0.046		
	620	0.099	0.062	0.046	0.041	0.046		
	820	0.209	0.122	0.088	0.048	0.024		
0.5M Fe^{2+}	360	0.0017	0.0019	0.0020	0.0016	0.0017		
	375	0.0049	0.0052	0.0052	0.0048	0.0069		
	392.5	0.0083	0.0091	0.0089	0.0077	0.0083		
0.1M Fe^{2+} + 0.5M Ce^{3+}	368	0.381	0.360	0.352	0.289	0.241		
	392.5	0.336	0.321	0.301	0.269	0.164		

10^{-7} s this band is stronger by 30% when 0.5 M Ce^{3+} is present than when 0.5 M Ce^{4+} is present, and that in the latter case this absorption completely dissappears in the course of a period 10^{-1} s following the pulse, are strong indications of this band being associated with an electron-excess center e^- rather than with a hole center h^+. The apearance of a transient electron center at the region around 800nm agrees very well with similar observations in a variety of oxide glasses[13,14]

The observation that in the presence of 0.5 M Fe^{2+} the low-wavelength absorption band does not appear provides very strong support for the assignment of the corresponding band in the case of 0.5 M Ce^{3+} to the formation of Ce^{4+}. No Fe^{3+} is observed to form, as indicated by the non-appearance of the characteristic sharp band at 375nm. The results obtained with 0.5 M Fe^{3+} show that the absorbance at 820nm is initially smaller by a factor of 2.5 than when the same level of Ce^{4+} is present. This probably means that Fe^{3+} is more reactive than Ce^{4+} towards the precursor of the stabilized electron-excess center. However, at long times the residual absorption observed in the Fe^{3+} glass is higher than in the case of the Ce^{4+} glass, and this residual absorption is probably due to Fe^{2+} which has a much lower absorptivity in the high wavelength range than e^-. The latter assumption is backed by a large body of data which indicate that the molar absorptivity of electron centers solvated in various media is usually in excess of 10^4 M^{-1} cm^{-1} in the 800nm peak region.[15]

The results obtained in the two combined systems are not indicative of any significant extent of reaction between Ce^{4+} and Fe^{2+} over the time range explored (10^{-7} s--10^{-1} s). In the case of the reduced system, the results obtained in the low-wavelength range in 0.1 M Fe^{2+} + 0.5 M Ce^{3+} are not significantly different from those obtained in 0.5 M Ce^{3+}, reflecting the formation of relatively stable Ce^{4+}; the results obtained in the high-wavelength range in 0.1 M Ce^{4+} + 0.5 M Fe^{3+} are practically identical with those obtained in 0.5 M Fe^{3+} alone, reflecting the depressed yield of stabilized e^- in the presence Fe^{2+} and the probable presence of residual absorption due to Fe^{2+}.

On the whole, the high-silica glass appears to be a medium where reactions involving radiation-produced species are much less noticeable than other oxide glasses. For instance, comparison of the yield of the stabilized e^- center based on observations of the initial absorption at 820nm in 0.5 M Ce^{3+}, 0.5 M Ce^{4+} and 0.5 M Fe^{3+} glasses, respectively indicate that 0.5 M Ce^{4+} scavenges only 30%, and 0.5 M Fe^{3+} only 88%, of the active electron-excess precursor. In phosphate glasses, mild oxidizing agents (Ag^+, Tl^+, Cd^{2+}, Pb^{2+}) react with 50% of the reactive e^- at a concentration of 0.05 M, and with 99.9% at a concentration of 0.5 M[13]. The conversion of Fe^{2+} to Fe^{3+} due to trapping of hole centers and the reaction between Ce^{4+} and Fe^{2+} are not observed at all in the high-silica matrix. This is probably due to the high rigidity and network density of this matrix compared with those of oxide glasses with a higher network modifier (e.g. alkali) content, and a lower network former content. Another

manifestation of the highly bonded, uninterrupted nature of the matrix is the small intensity of the radiation-induced absorption in high-silica glasses as compared with the intensity observed in alkali silicate glasses under comparable doses. Dopants such as Ce and Fe are probably trapped in matrix-forming sites rather than on non-bridging oxygen sites, resulting in a much smaller reactivity, for instance in redox processes such as the ones studied here. It should be noted that the spectral characteristics of absorption and emission bands due to dopants are much less susceptible to the introduction of small amounts of basic or acidic additives in high-silica glasses than in alkali silicate glasses, probably for the same reason.

From an applied point of view, the findings summarized in Table IV indicate that at room temperature, over the period studied so far (10^{-7} s--10^{-1} s after the irradiation pulse), the introduction of Ce is not shown to be useful in suppressing the radiation-induced absorption band due either to centers associated with the high-silica matrix itself or to centers originating in the presence of Fe impurities. An extension of the present studies to a longer time scale is likely to be very useful in establishing whether Ce is more efficient in reducing the intensity of the residual, "permanent" radiation-induced absorption. As a more immediate objective, we believe that extension of the studies on the oxidized samples listed in Table IV, to the low wavelength region as well as extension of the studies on the Fe^{2+} - containing samples to the high-wavelength region could go a long way towards substantiation of the conclusions

reported above with respect to the nature of the radiation-produced species.

IV Fluoride Glasses

A. Introduction

Glasses based on ZrF_4 and HfF_4 show excellent potential as materials for optical components operating in the mid-IR (2-5 μm)[16,17]. Earlier glasses of this type were primarily based on ZrF_4. A recent investigation[18] showed, however, that glasses based on the heavier HfF_4, which is otherwise virtually identical chemically to ZrF_4, were apt to be transparent out to longer wavelengths than the corresponding ZrF_4-based glasses. In this section we describe a systematic investigation of the glass forming region in the HfF_4-BaF_2-LaF_3 system. In addition a study of glass formation in HfF_4-based glasses containing a number of other components has been carried out, along with differential scanning calorimetry (DSC) determinations of glass transition and crystallization temperatures of a number of compositions based on either ZrF_4 or HfF_4.

B. Experimental Procedure

Chemicals used in glass synthesis were as follows:

HfO_2 (9%, Teledyne Wah Chang Albany for earlier melts; 99.999%, Apache Chemical, Inc. for later melts)

ZrO_2 (99+%, Alfa Products)

BaF_2 (99%, Alfa Products)

La_2O_3 (99.999%, Aldrich Chemical co.)

PbF_2 (98%, Alfa Products)

Gd_2O_3 (99.9%, Alfa Products)

CsF (99.9%, Alfa Products)

Al (99.9% metallic powder, Alfa Products)

$NH_4F \cdot HF$ (Alfa Products)

During the earlier parts of this study the glass synthesis procedure was varied somewhat from melt to melt, in an effort to improve the procedure. The majority of the glasses were prepared using the following method, which we found to be optimum at that time.

A glass batch (typically ~ 20g) consisting of the metal oxides, metal fluorides and Al metal calculated to give the final desired fluoride glass composition was weighed into a plastic jar. 20g $NH_4F \cdot HF$ was then added and thoroughly mixed with the batch. The $NH_4F \cdot HF$ converts oxides to fluorides via reactions of the form:

$$HfO_2(s) + 4\ NH_4F \cdot HF(s) \xrightarrow{300\text{-}400^\circ C}$$

$$HfF_4(s) + 2\ H_2O(g) + 4\ NH_4F(g)$$

Al metal presumably reacts with O_2 in the furnace atmosphere and then undergoes fluoridation.

Fluoridation and melting were carried out in a Hoskins crucible furnace. A flow of dry N_2 gas through the furnace was maintained by introducing a N_2 stream through a Vycor glass tube entering through the furnace bottom. The top of the furnace was closed with a cover made of Transite or Marinite; the cover

contained two small holes for insertion of a chromel-alumel thermocouple to monitor furnace temperature and to allow escape of water vapor and NH_4F and ZrF_4 particulates formed from vapors from the reaction mixture.

The batch was placed in a 100 ml Pt crucible loosely covered with a Pt lid and placed in the furnace for 1h at about 320°C to allow fluoridation to occur. The crucible was then removed from the furnace and the hot crystalline mixture broken up with a Pt rod. To ensure complete flouridation, an additional 20g $NH_4F \cdot HF$ was then mixed in with the fluorides and the loosely covered crucible replaced in the furnace at 320°C. The furnace temperature was raised to about 760°C at a rate of about 15°C/min, held there until heavy evolution of NH_4F fumes had abated, and then heated at 760°C for an additonal 10 min.

At this point the fluoride mixture should be completely molten. However the Pt crucible may have volatilized solid ZrF_4 deposits on the cooler parts of the inner walls. In order to avoid contaminating the melt with these solid particles during casting, the melt was poured into a clean 25 mL Pt crucible, 10g $NH_4F \cdot HF$ added to the surface, and the loosely covered crucible replaced in the furnace at 760°C. It was again heated until heavy fume evolution had stopped plus an additional 10 min and removed briefly from the furnace for inspection. The melt at this point was usually clear; if it had a grayish color (probably due to the presence of lower valent metallic cations), it was reheated at 760°C for an additional 5-10 min. This generaly caused the melt to become clear, presumably by oxidation of the

lower valent species, since oxygen had been admitted to the furnace atmosphere in removing the melt for inspection.

The melts were cast into rectangular glass pieces a few mm thick by pouring them into a mold at room temperature formed by arranging four brass bars on a brass sheet. After filling the mold with the melt, the surface was quenched by quickly placing a brass sheet on top of the melt. In cases where the melt devitrified during this casting procedure, an attempt was made to form very thin glass sheets by rapid quenching; a small amount of melt was poured onto a brass plate and a second plate quickly placed on top of it.

After casting, glass specimens were immediately placed in a muffle furnace preset to an appropriate temperature for annealing (300°C). After isothermal annealing for a brief time, the furnace was turned off and the glasses allowed to cool to room temperature inside the furnace.

DSC scans were carried out using a Perkin-Elmer Model DSC-2 differential scanning calorimeter on a large number of specimens to determine the glass transition temperatures, Tg, and the temperatures of onset of crystallization, T_x, during heating. The DSC samples were contained in gold sample pans, and a heating rate of 10°C/min was employed.

C. Results and Discussion

1. Glass-Forming Region in the HfF_4-BaF_2-LaF_3 System

In Fig. 2 is shown the glass-forming region in the system HfF_4-BaF_2-LaF_3 as determined in a preliminary study during the very early part of this project. (Compositions in Fig. 2 and in the remainder of this report are given in mole percent metal fluorides.) In this region crystal-free glass specimens a few mm thick could be cast. Fig. 2 also shows for comparison the glass-forming region in the ZrF_4-BaF_2-LaF_3 system, as reported by Lecoq, Poulain and Lucas[19]. As expected from the chemical and physical similarities between HfF_4 and ZrF_4, the two glass-forming regions are also very similar.

Fig. 2. Comparison of glass-forming regins in HfF_4-BaF_2-LaF_3 and ZrF_4-BaF_2-LaF_3 systems.

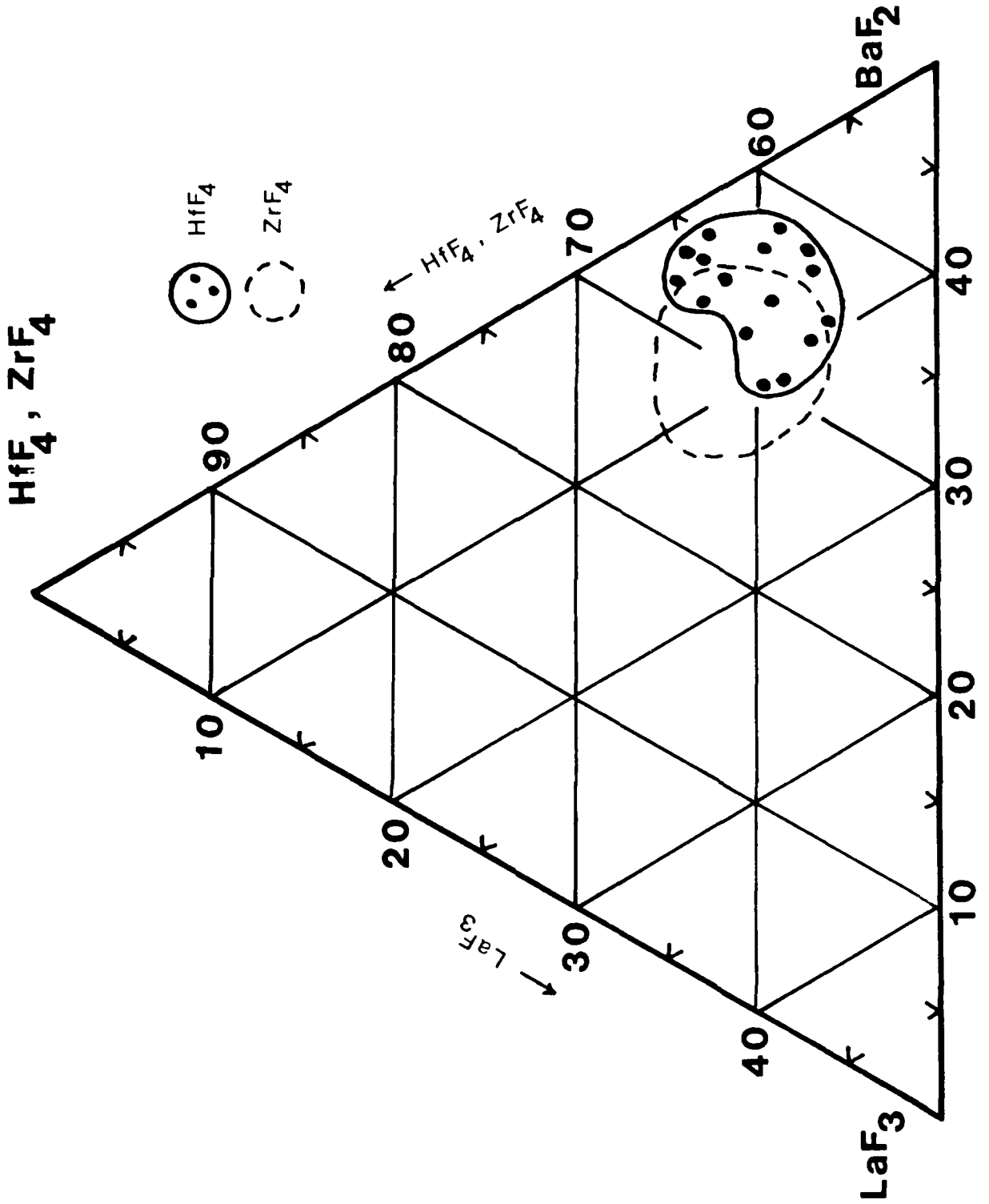
HfF_4, ZrF_4
HfF_4
ZrF_4
← HfF_4, ZrF_4
BaF_2
LaF_3
LaF_3 →
90
80
70
60
40
30
20
10
10
20
30
40

2. More Recent Glass-Formation Studies

Table V lists the fluoride melts studied for glass formation during the later parts of this project; these were all prepared using the melting procedure described previously. The comments in the "Results" column indicate the following:

"Very good glass"	Glasses of good quality, inclusion-free to the eye, could be cast in thicknesses up to 3.5 mm.
"Glass"	Glasses containing a few crystalline inclusions or with slight surface devitrification could be cast in thicknesses up to 3.5 mm.
"Glass on fast quenching"	Only thin glass specimens (< 1 mm) could be prepared by quenching between two brass plates; thicker samples showed substantial devitrification.
"Not a glass"	Even melts subjected to fast quenching were largely or wholly devitrified.

The optimum composition for glass formation in the HfF_4-BaF_2-LaF_3 system is roughly 62 HfF_4-33 BaF_2-5 LaF_3. As shown in Table V, up to 10 mole% of the BaF_2 may be replaed by CsF and up to 18 mole% of the BaF_2 may be replaced by PbF_2 with no great sacrifice in glass quality. Replacement of BaF_2 by both CsF and PbF_2 is also possible. Small amounts of AlF_3 can be incorporated into these last glasses.

C. Thermal Analysis

In Fig. 3 is shown a typical DSC scan at a 10°C/min heating rate. Tg, the glass transition temperature, marks the temperature region in which the glass begins to exhibit liquid-like properties and corresponds to a shear viscosity of 10^{11}-10^{12} Pa•s (10^{12}-10^{13} P). The glass

TABLE V. Fluoride compositions tested for glass formation at Catholic University of America

Sample No.	Composition (mol %)								Results
	HfF_4	LaF_3	AlF_3	BaF_2	PbF_2	CsI	GdF_3	ZrF_4	
28/11	60	10	-	30	-	-		-	Glass
30/11	60	5	-	35	-	-	-	-	Glass
29/11	57.50	8.75	-	33.75	-	-	-	-	Glass
3/12	60	10	-	30	-	-	-	-	Glass
4/12	55	5	-	40	-	-	-	-	Not a glass
5/12	60	-	-	40	-	-	-	-	Glass on fast quenching
6/12	65	5	-	30	-	-	-	-	Glass on fast quenching
11/12	62	3	-	35	-	-	-	-	Glass
12/12	62	8	-	30	-	-	-	-	Glass on fast quenching
13/12	65		-	35	-	-	-	-	Glass on fast quenching
7/1	62	5	-	28	-	5	-	-	Very good glass
15/1	62	5	-	23	-	10	-	-	Very good glass
16/1	62	5	-	26	-	7	-	-	Very good glass
17/1	62	5	-	25	3	5	-	-	Very good glass
21/1	62	5	-	30	-	3	-	-	Very good glass
23/1	62	5	-	27	1	5	-	-	Very good glass
20/3	62	5	-	15	10	8	-	-	Very good glass
21/3	62	5	-	-	23	10	-	-	Glass
26/3	65	5	-	10	12	8	-	-	Very good glass
31/3	62	5	15	10	-	8	-	-	Not a glass
1/4	62	5	5	10	10	8	-	-	Not a glass
2/4	62	5	2	15	10	6	-	-	Very good glass
3/4	62	5	-	15	18	-	-	-	Glass
8/4	62	-	-	15	15	8	-	-	Very good glass
9/4	62	-	2	15	15	6	-	-	Not a glass
10/4	62	5	-	15	10	8	-	-	Very good glass
17/4	62	5	-	33	-	-	-	-	Very good glass
3/6	62	10	-	10	10	8	-	-	Glass on fast quenching
5/6	62	10	-	28	-	-	-	-	Very good glass
6/6	62	-	-	38	-	-	-	-	Glass
9/6	60.3	-	-	27.2	-	12.5	-	-	Glass on fast quenching
12/6	62	-	-	30	-	8	-	-	Glass
16/6	62	5	-	-	23	10	-	-	Glass
17/6	62	5	-	-	25	8	-	-	Not a glass
6/3	62	-	-	25	-	5	8	-	Glass on fast quenching
27/3	65	-	-	12	10	8	5	-	Glass on fast quenching
16/5	-	5	-	33	-	-	-	62	Very good glass

Fig. 3. DSC scan at 10°C/min heating rate of 58 HfF_4-33 BaF_2-9LaF_3 glass. Glass transition temperature, Tg, and temperature of onset of crystallization during heating, T_x are indicated.

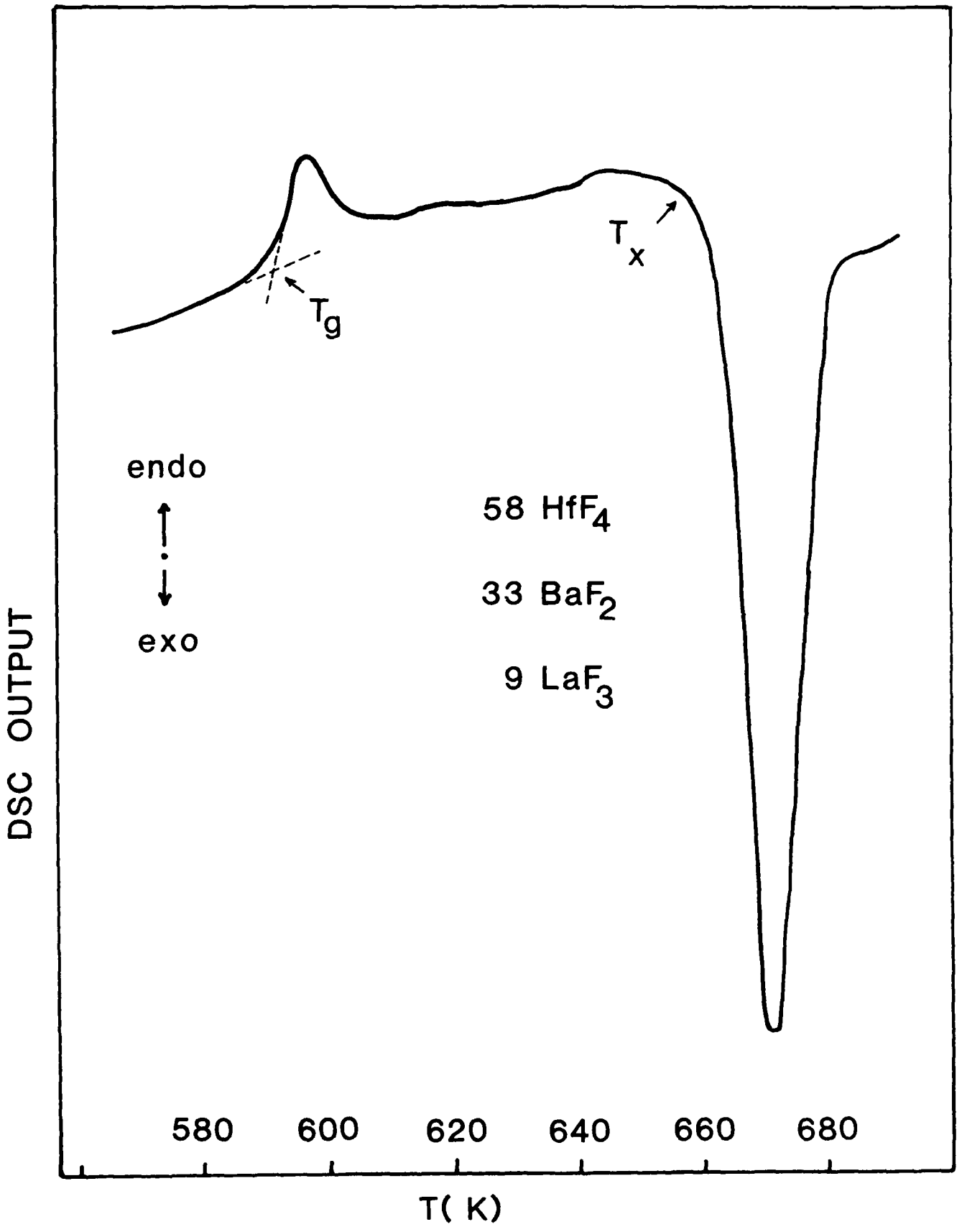
T_g
T_x
endo
exo
58 HfF_4
33 BaF_2
9 LaF_3
DSC OUTPUT
580
600
620
640
660
680
T(K)

annealing temperature should be chosen to be a few degrees below Tg. Crystallization of the glass during heating above Tg is marked by a substantial exothermic peak in the DSC scan; T_x is the onset temperature of this crystallization exotherm. T_x presumably marks the temperature at which the viscosity of the melt becomes low enough that crystal growth can proceed at a substantial rate. Numerous workers have sugggested a correlation between the separation of Tg and T_x and the glass forming ability of the melt. Melts with larger values of (T_x-Tg) are expected to be better glass formers.

In Table VI are given Tg and T_x values for a large number of the glasses listed in Table V. Samples number 10/4(22/4) and 10/4(23/4) are separately melted glass batches of the same composition, as are samples number 16/5, 16/5(20/5) and 16/5(21/5). There is excellent agreement among the Tg and T_x values measured for samples of the same composition from different batches.

Tg's for all of the glasses in Table V are quite similar, i.e., ~ 300°C. Addition of either or both CsF or PbF_2 at the expense of BaF_2 to a HfF_4-BaF_2-LaF_3 glass appears to lead to small decreases in Tg.

In Table VII we have compared the (T_x-Tg) values of Table VI with the qualitative observations of glass-forming ability presented in Table V. There seems to be a fair correlation, such that melts which form a "very good glass" tend to have the larger $(Tg-T_x)$ values. Addition of CsF and PbF_2 to HfF_4-BaF_2-LaF_3 glasses increases (T_x-Tg), an expected improvement in glass-forming ability on increasing the number of melt

TABLE VI. Glass transition temperature Tg and temperatures of onset of crystallization, Tx, at 10°C/min heating rate for fluoride glasses melted at Catholic University of America

Sample No.	Composition (mol %)									
	ZrF_4	HfF_4	LaF_3	GdF_3	AlF_3	BaF_2	PbI_2	CsF	Tg(°C)	Tx(°C)
30/11	-	60	5	-	-	35	-	-	315	389
11/12	-	62	3	-	-	35	-	-	319	391
17/4	-	62	5	-	-	33	-	-	312	395
21/1	-	62	5	-	-	30	-	3	311	382
7/1	-	62	5	-	-	28	-	5	316	390
16/1	-	62	5	-	-	26	-	7	313	398
15/1	-	62	5	-	-	23	-	10	306	391
23/1	-	62	5	-	-	27	1	5	313	393
20/3	-	62	5	-	-	15	10	8	295	392
10/4 (22/4)	-	62	5	-	-	15	10	8	295	393
10/4 (23/4)	-	62	5	-	-	15	10	8	295	393
26/3	-	65	5	-	-	10	12	8	296	390
8/4	-	62	-	-	-	15	15	8	277	340
3/4	-	62	5	-	-	15	18	-	292	362
2/4	-	62	5	-	2	15	10	6	309	427
16/5	62	-	5	-	-	33	-	-	305	380
16/5 (20/5)	62	-	5	-	-	33	-	-	309	372
16/5 (21/5)	62	-	5	-	-	33	-	-	304	379
6/3	-	62	-	8	-	25	-	5	304	377
27/3	-	65	-	5	-	12	10	8	286	349

TABLE VII. Correlation between qualitative observations of glass-forming ability (Table I) and (T_x-Tg) (Table II).

Sample No.	(T_x-Tg) (°C)	Glass-forming ability
2/4	118	Very good glass
10/4	98 ave	Very good glass
20/3	97	Very good glass
26/3	94	Very good glass
15/1	85	Very good glass
16/1	85	Very good glass
17/4	83	Very good glass
23/1	80	Glass
7/1	74	Very good glass
30/11	74	Glass
6/3	73	Glass on fast quenching
11/12	72	Glass
16/5	71 ave	Very good glass
21/1	71	Very good glass
3/4	70	Glass
8/4	63	Very good glass
27/3	63	Glass on fast quenching

components. The largest value to (T_x-Tg) in Table II is for sample no. 2/4 containing 2 mole% AlF_3; small AlF_3 additions appear to enhance glass formation in these melts. The two glasses (nos. 6/3 and 27/3) in which LaF_3 has been replaced by GdF_3 having fairly low (T_x-Tg) values and form glasses only on fast quenching, suggesting that GdF_3 is deleterious to glass formation in these systems.

In Table VIII are listed Tg and T_x values for a number of ZrF_4- or HfF_4-based glasses containing between four and nine components. These were melted by Dr. Martin Drexhage of the Solid State Sciences, RADC, Hanscom AFBMA, using techniques very similar to those employed by us. The Tg and (T_x-Tg) values are comparable to those for the Catholic University glasses listed in Table VI. It appears that one reaches a point of diminishing returns in enhancement of glass-forming ability by going to a very large number of components, particularly if these are different alkali flourides.

D. -OH Impurities

1. Introduction

Recently synthesized glasses based on ZrF_4 and HfF_4[18-20] exhibit considerable promise as ultrahigh transparency materials for the mid-IR (2 - 5μm)[16/18,21]. One source of extrinsic absorption in this regin is a peak at 3400 cm^{-1} (2.9μm) due to hydroxyl groups[17,22]. Preliminary results[17] indicated that a substantial part of the -OH giving rise to this peak might lie on the surface rather than in the bulk of the glass. To separate contributions from surface and bulk -OH absorption, we have

TABLE VIII Glass transition temperatures Tg and temperatures of onset of crystallization, T_x, at 10°C/min heating rate for fluoride glasses melted at Solid State Sciences Div., RADC, Hanscom AFB, MA.

Sample No.	ZrF_4	HfF_4	BaF_2	ThF_4	LaF_3	LiF	NaF	KF	RbF	CsF	LuF_3	Tg(°C)	T_x(°C)	(T_x-Tg)(°C)
ZBTLNRC-063	53	-	22	7.7	4.2	-	4.37	-	4.37	4.37	-	296	384	88
ZBTKLuRC-045	53	-	22	7.7	-	-	-	4.37	4.37	4.37	4.2	300	376	76
ZBTKLRC-058	53	-	22	7.7	4.2	-	-	4.37	4.37	4.37	-	304	382	78
ZBTLRC-046	57.37	-	22	7.7	4.2	-	-	-	4.37	4.37	-	303	402	99
ZBLC-033	60	-	27.5	-	7.5	-	-	-	-	5	-	300	374	74
HBTLKLNRC-062	-	53	22	7.7	4.2	2.62	2.62	2.62	2.62	2.62	-	298	397	99
HBTKLRC-059	-	53	22	7.7	4.2	-	-	4.37	4.37	4.37	-	312	389	77
HBTLNRC-065	-	53	22	7.7	4.2	-	4.37	-	4.37	4.37	-	302	403	101
HBLC-029	-	56	22.5	-	6.5	-	-	-	-	15	-	295	375	80
HBLR-028	-	56	22.5	-	6.5	-	-	-	15	-	-	299	367	68

measured the intensity of the 3400 cm^{-1} peak as a function of thickness for several ZrF_4- and HfF_4-based glasses melted under varying conditions.

2. Experimental Procedure

Six glasses in the ZrF_4-BaF_2-LaF_3 or HfF_4-BaF_2-LaF_3 systems, with compositions near the middle of the respective glass-forming regions[16,17,19], were synthesized. Starting materials were ZrO_2 or HfO_2, BaF_2 and La_2O_3 or LaF_3, all of > 99% purity, mixed with an excess of $NH_4F \cdot HF$. Melting procedures were similar to those described previously[17,18]. Four batches were exposed only to N_2 atmosphere during melting; two were subjected to a reactive atmosphere of CCl_4[22] entrained in Ar during the last stage of melting. Designations of the glasses (HBL-1, ZBL-1, etc.), batch compositions and melting atmospheres are given in Table IX.

The glasses were cast into thin plates a few mm thick and annealed. The plates were given a rough polish* on the oppposite faces with Sic paper using lapping oil as a lubricant. Final stages of polishing were done with 5μm and 0.05 μm Al_2O_3 using water as a lubricant, except in one case described below. After polishing, the plates were wiped clean with lens tissue moistened with methanol and their IR spectra** recorded both on a normal transmission scale and on a transmission scale expanded

---

* Minimet Polisher, Buehler Ltd., Evanstan, IL

** Model 467 IR Spectrometer, Perkin Elmer Corp., Norwalk, CT

Table IX Compositions, melting conditions and thickness dependence of absorption loss at 3400 cm^{-1} -OH peak for fluorozirconate and fluorohafnate glasses.

Glass	Composition (mol %)	Melting atm	α_{bulk} (cm^{-1})	B	Std. Dev.
HBL-1	60 HfF_4-35 BaF_2-5 LaF_3	N_2	0.19	0.008	0.006
HBL-2	62 HfF_4-33 BaF_2-5 LaF_3	CCl_4	0.01	0.008	0.003
ZBL-1	62 ZrF_4-33 BaF_2-5 LaF_3	N_2	0.08	0.001	0.001
ZBL-2	62 ZrF_4-33 BaF_2-5 LaF_3	N_2	-0.01	0.012	0.003
ZBL-3	62 ZrF_4-33 BaF_2-5 LaF_3	CCl_4	0.01	0.006	0.002
ZBL-4	62 ZrF_4-33 BaF_2-5 LaF_3	N_2	---	---	---

5X. Following this one of the glass plates (ZBL-4) was left mounted on its IR spectrometer specimen holder and its spectrum remeasured periodically for one month. During this time the glass was covered loosely so that it was protected from dust, but otherwise exposed to the ambient laboratory atmosphere. The other five glass plates were reduced in thickness in several stages using the polisher; the IR spectrum was recorded for each thickness. For one of these glasses (HBL-1) water and lapping oil were used alternately as lubricants during the final stage of polishing to assess any effects of the lubricant on the intensity of the -OH absorption.

3. Results and Discussion

Figure 4 shows a typical IR spectrum. The upper spectrum, from 1000 to 4000 cm^{-1}, has been measured on the normal scale for transmission, T; the discontinuity at about 2000 cm^{-1} is due to a grating change. The lower spectrum, from 2000 to 4000 cm^{-1}, was measured on a transmission scale expanded 5X. The gradual decrease in transmission below 2200 cm^{-1} is due to intrinsic multiphonon absorption and has been discussed elsewhere[16-18]. The weak, poorly resolved absorption bands at about 2900 cm^{-1} are from C-H vibrations of organic surface contaminants[17]. Finally, the prominent broad absorption peak at about 3400 cm^{-1} is due to -OH.

Fig. 5 shows expanded scale IR spectra in the vicinity of the -OH peak for different thicknesses, x, of two glasses. The intensity of the -OH absorption on the expanded scale is designated by $(T_{o,ex}-T_{ex})$, where $T_{o,ex}$ is the measured transmission in a flat region of the spectrum where apparent losses are due

Fig. 4. Ir spectrum of 60 HfF_4-35 BaF_2-5 LaF_3 glass (HBL-1) 0.185 cm thick on normal and 5X expanded transmission scales.

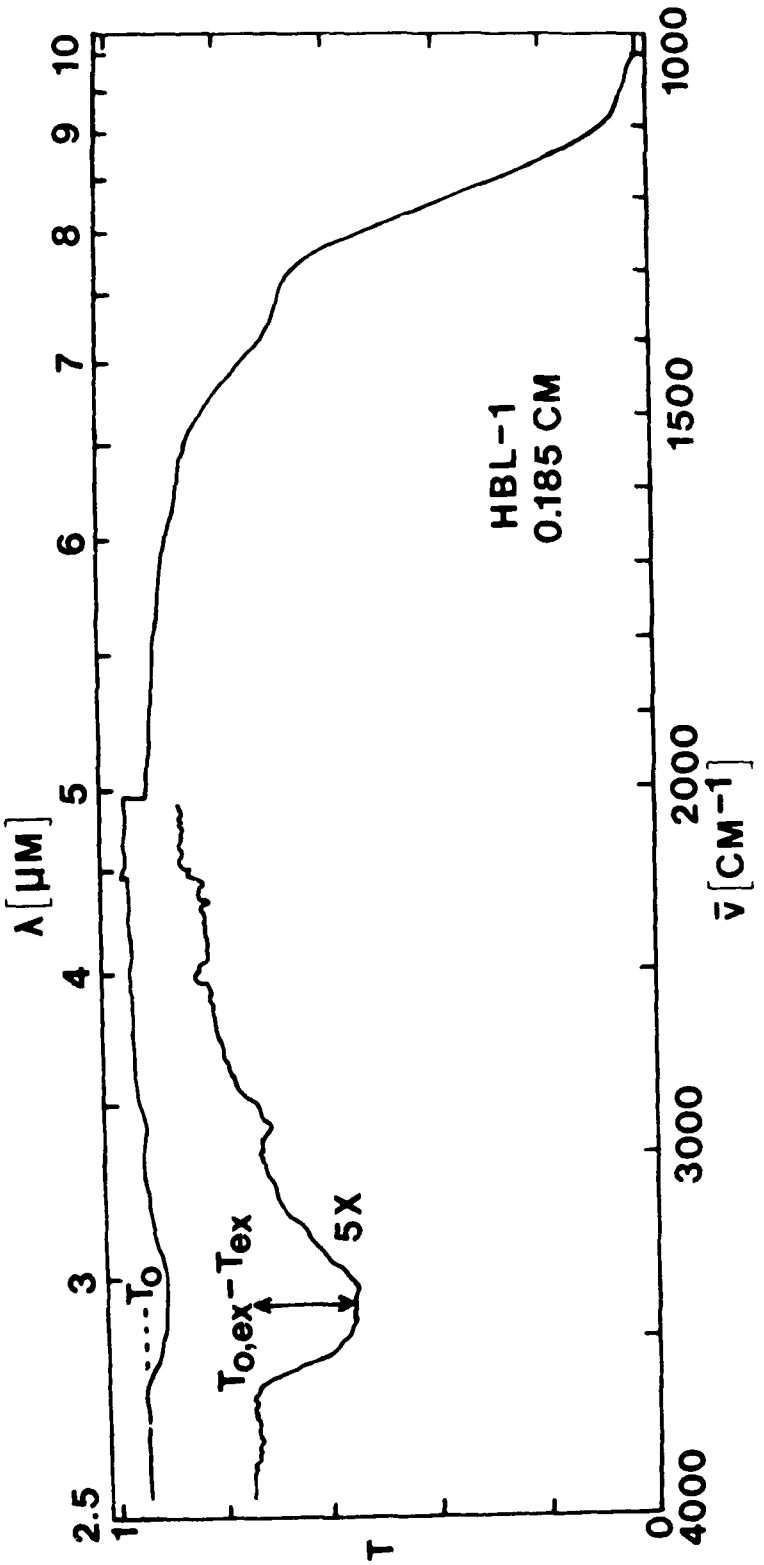
λ[μM]
2.5
1
3
4
5
6
7
8
9
10
T
0
4000
3000
2000
1500
1000
ν̄[CM⁻¹]
HBL-1
0.185 CM
T_o
T_o,ex − T_ex
5X

Fig. 5. 5X expanded scale IR spectra in the vacinity of the -OH absorption peak for different thicknesses of 60 HfF_4-35 BaF_2-5 LaF_3 (HBL-1) and 62 HfF_4-33 BaF_2-5 LaF_3 (HBL-2) glasses.

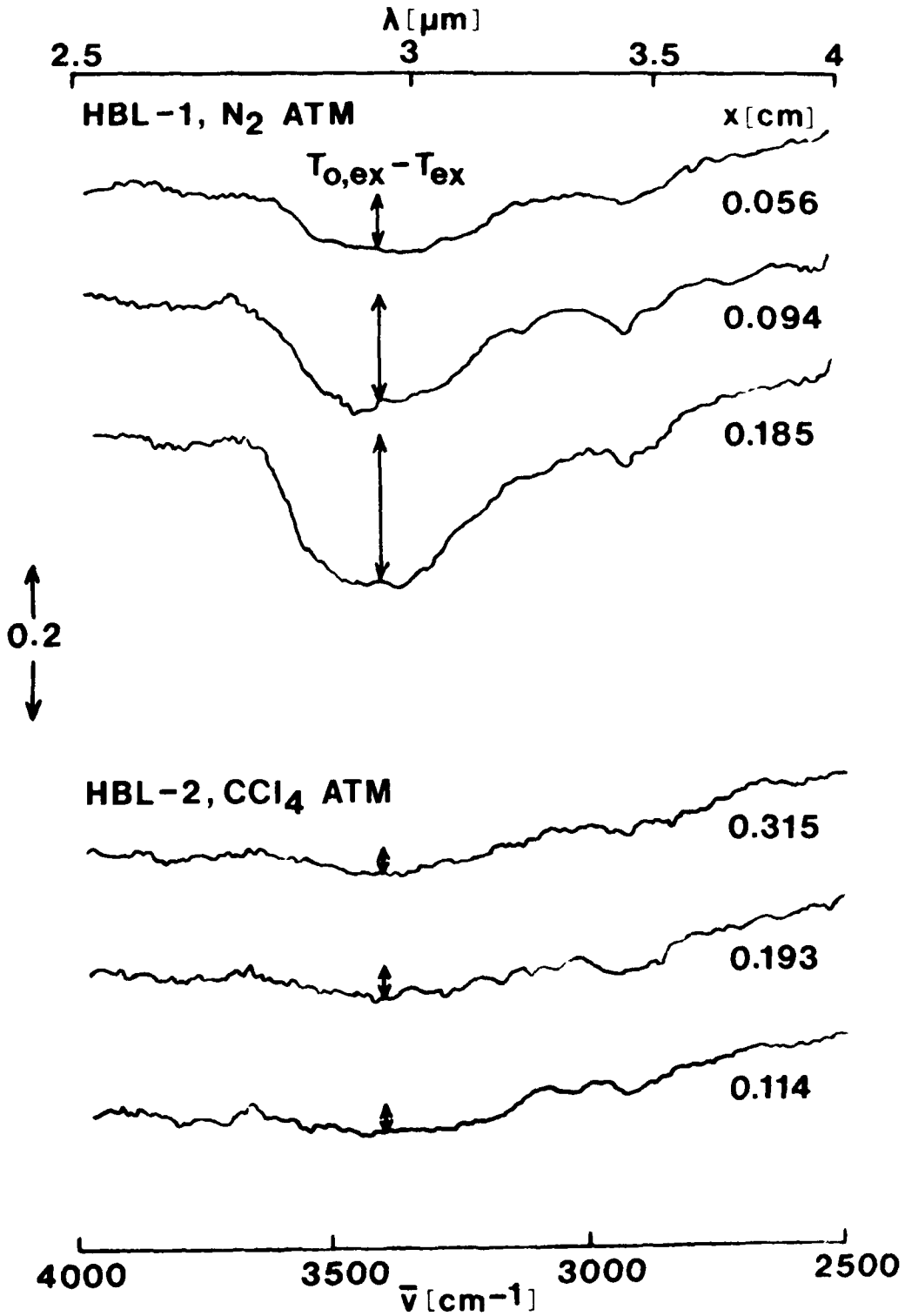
λ[μm]
2.5
3
3.5
4
HBL-1, N2 ATM
x[cm]
To,ex - Tex
0.056
0.094
0.185
0.2
HBL-2, CCl4 ATM
0.315
0.193
0.114
4000
3500
3000
2500
ν̄[cm-1]

only to reflection, and T_{ex} the measured transmission at the 3400cm^{-1} peak. For the HBL-1 glass, melted only under N_2 atmosphere, $(T_{o,ex}-T_{ex})$ decreases with decreasing thickness, indicating that a substantial amount of the -OH responsible for the 3400 cm^{-1} peak is contained in the bulk of the glass. For the HBL-2 glass, melted under CCl_4 atmosphere, $(T_{o,ex}-T_{ex})$ is much smaller than for the HBL-1 glass and independent of thickness within experimental error. Hence the amount of -OH in the HBL-2 glass is much smaller than in the HBL-1 glass and is situated primarily on the surface.

In a case in which both surface and bulk components contribute to a weak absorption band, the dependence of the band intensity on sample thickness, x, should be given to a good approximation by

$$\ln(T_o/T) = \alpha_{bulk}x + B \qquad (1)$$

where T is the transmission at the absorption peak measured on the normal spectrometer scale, T_o the normal scale transmission in an adjacent spectral region where only reflectivity losses occur (cf. Fig. 1), α_{bulk} the absorption coefficient at the peak due to material in the bulk of the specimen, and B the contribution to $\ln(T_o/T)$ from surface material. For our glasses T at the 3400 cm^{-1} peak was evaluated from the 5X expanded scale spectra via the expression:

$$T = T_o - (T_{o,ex}-T_{ex})/5 \qquad (2)$$

In Figs. 6 and 7 $\ln(T_o/T)$ is plotted versus glass thickness for the five glass specimens. The lines are least squares fits to Eq. (1); the corresponding least squares parameters are given in Table IX. Standard deviations from the fits are of the order of the estimated experimental uncertainity in $\ln(T_o/T)$, ±0.004. The uncertainty in the 3400 cm^{-1} bulk -OH absorption coefficient, α_{bulk}, evaluated by this method is roughly ± 0.01 cm^{-1}.

For the glasses (HBL-1, ZBL-1, ZBL-2) melted only under N_2 atmosphere, α_{bulk} is of variable magnitude, ranging from zero within experimental error to 0.19 cm^{-1}. Melting under inert atmosphere thus leaves a varied and uncontrolled amount of -OH in the bulk glass. On the other hand, α_{bulk} for the glasses (HBL-2, ZBL-3) melted under CCl_4 reactive atmosphere is zero within ±0.01 cm^{-1}. Hence this procedure, developed by Robinson et al.[22], appears to be a reliable method for purging the bulk melt of -OH. These authors[22] reported an absorption coefficient of 0.006 cm^{-1} measured calorimetrically with an HF laser at 2.8 μm (3600 cm^{-1}) for a 60 ZrF_4-33BaF_2-7 ThF_4. The intensity of the -OH peak at 3600 cm^{-1} is about half its value at 3400 cm^{-1}, so that our results for ZrF_4- or HfF_4-based glasses melted under CCl_4 would give an upper limit of about 0.005 cm^{-1} for the bulk -OH absorption at 3600 cm^{-1}. This is in good agreement with the results of Robinson et al.[22], presuming that their calorimetric method is sensitive primarily to bulk absorption.

Fig. 6. Thickness dependence of $\ln(T_o/T)$ at the 3400 cm^{-1} -OH peak for HfF_4-BaF_2-LaF_3 glasses

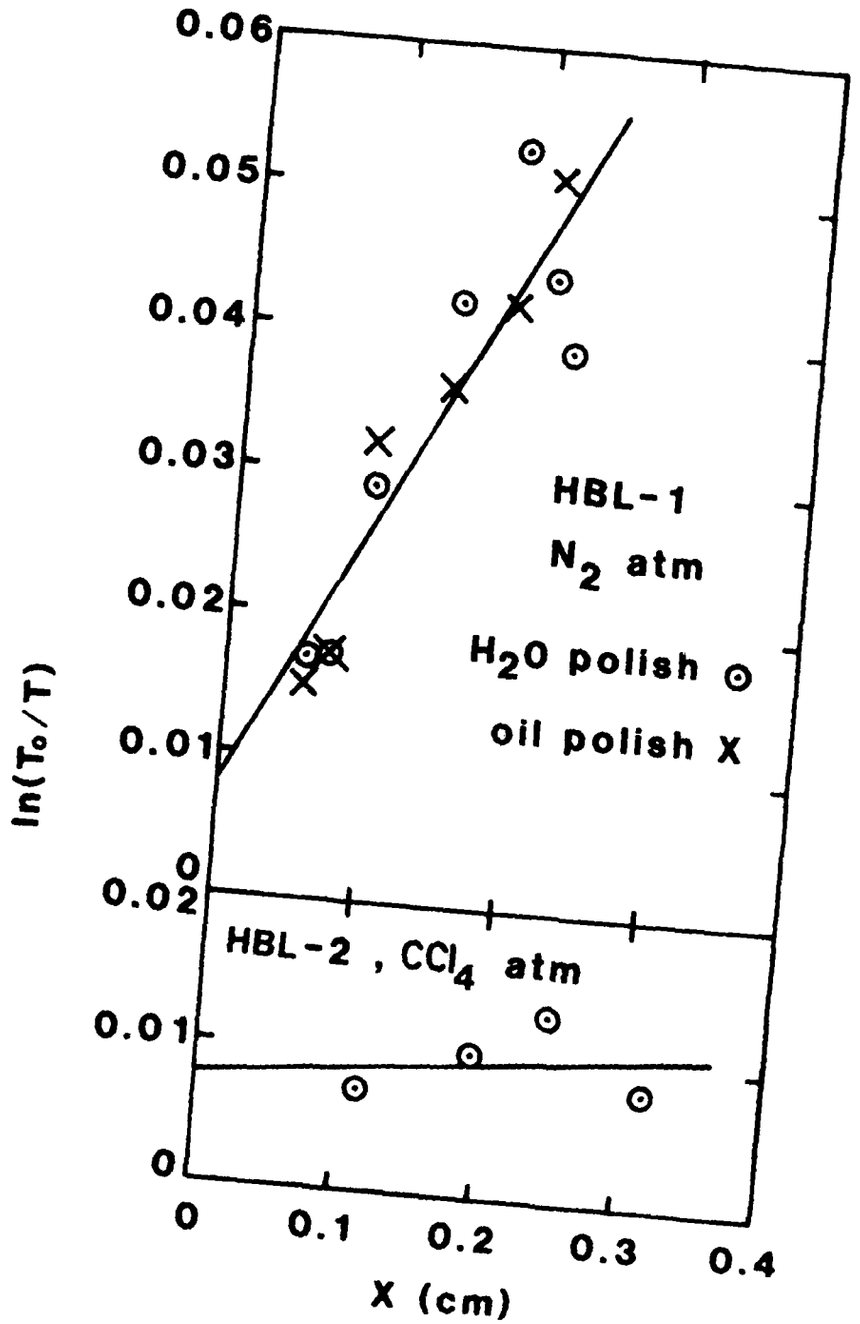
0.06
0.05
0.04
0.03
0.02
0.01
0
0.02
0.01
0
0
0.1
0.2
0.3
0.4
X (cm)
ln(T₀/T)
HBL-1
N₂ atm
H₂O polish ⊙
oil polish X
HBL-2 , CCl₄ atm

Fig. 7. Thickness dependence of $\ln(T_o/T)$ at the 3400 cm^{-1} -OH peak for ZrF_4-BaF_2-LaF_3 glasses

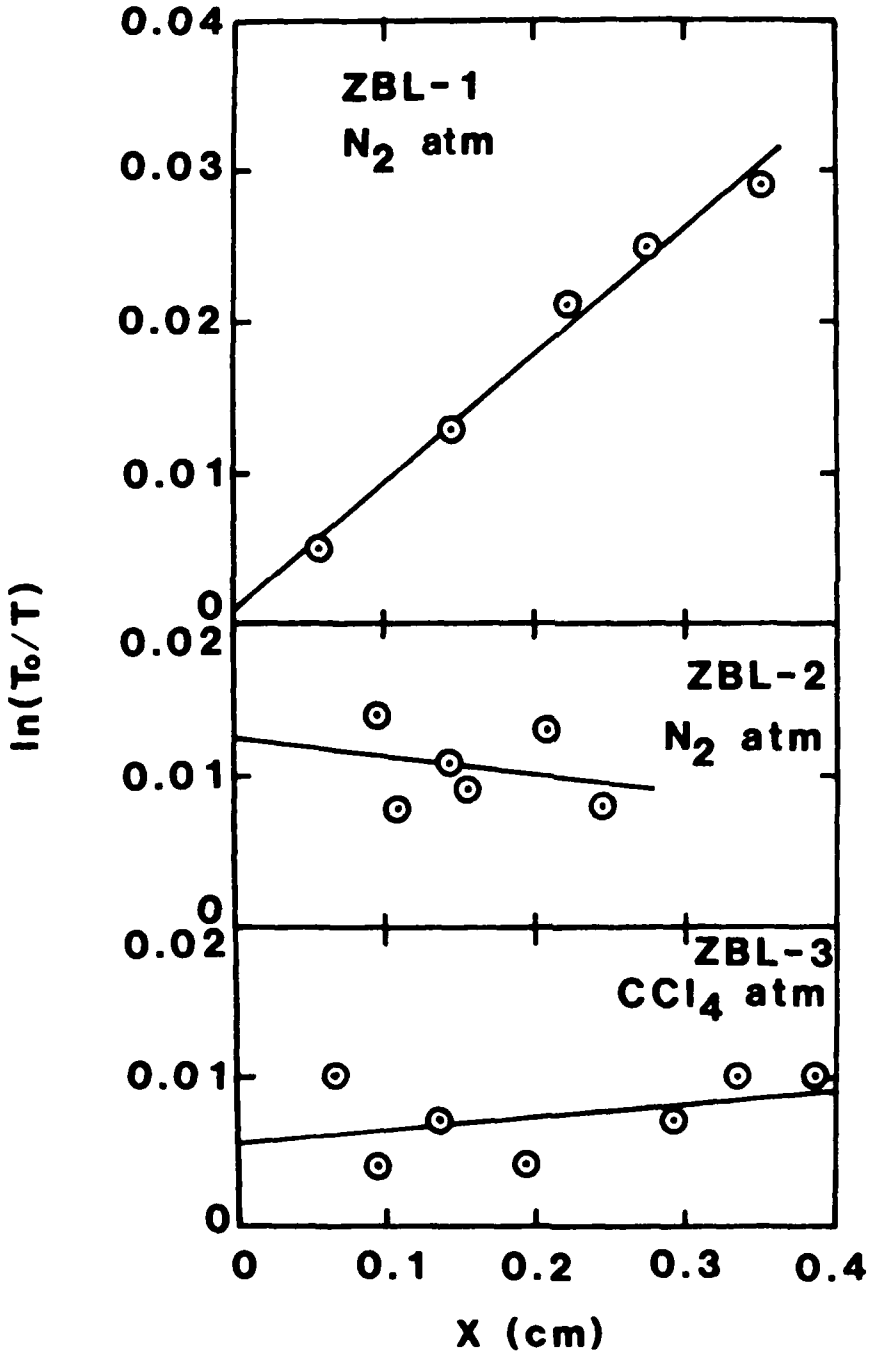
0.04
0.03
0.02
0.01
0
ZBL-1
N_2 atm
0.02
0.01
0
ZBL-2
N_2 atm
0.02
0.01
0
ZBL-3
CCl_4 atm
$\ln(T_o/T)$
0
0.1
0.2
0.3
0.4
X (cm)

Knowing the band shape of the -OH peak from glasses containing large amounts of -OH, our upper limit of about 0.01 cm^{-1} at 3400 cm^{-1} for the bulk -OH absorption coefficient in glasses melted under CCl_4 can be used to estimate bulk -OH absorption coefficients at other wavelengths for the latter glasses. For example, the intensity of the -OH band has dropped to about 10% of its peak value by 3000 cm^{-1}, so that at this frequency an upper limit of about 10^{-3} cm^{-1} can be set for the bulk -OH absorption coefficient of glasses melted under CCl_4.

As shown in Fig. 6 for the HBL-1 glass, the intensity of the -OH absorption band for a given thickness is independent of whether the final stages of polishing are done with lapping oil or with pure water as a lubricant. Consequently no special precautions need be taken to protect these glasses from water during polishing to avoid formation of surface films. Rather, it appears that the surface -OH observed in the IR spectum is produced after polishing by attack of environmental water on the fresh surface.

Figure 8 shows the time dependence of $\ln(T_O/T)$ at the 3400 cm^{-1} -OH peak for the ZBL-4 glass exposed to the ambient laboratory atmosphere over a 1 month period. The mean value of $\ln(T_O/T)$, shown by the dashed line, is 0.015 ± 0.004 cm^{-1}, and only one point in Fig. 8 departs by more than 2 standard deviations from this mean. Since the estimated experimental accuracy of $\ln(T_O/T)$ is also $\pm$ 0.004, there is no evidence of increase in thickness of the surface -OH layer due to attack by atmospheric water over this period. This underscores the

Fig. 8. Time dependence of $\ln(T_0/T)$ at the 3400 cm^{-1} -OH peak for 62 ZrF_4-33 BaF_2-5 LaF_3 glass exposed to ambient laboratory atmosphere.

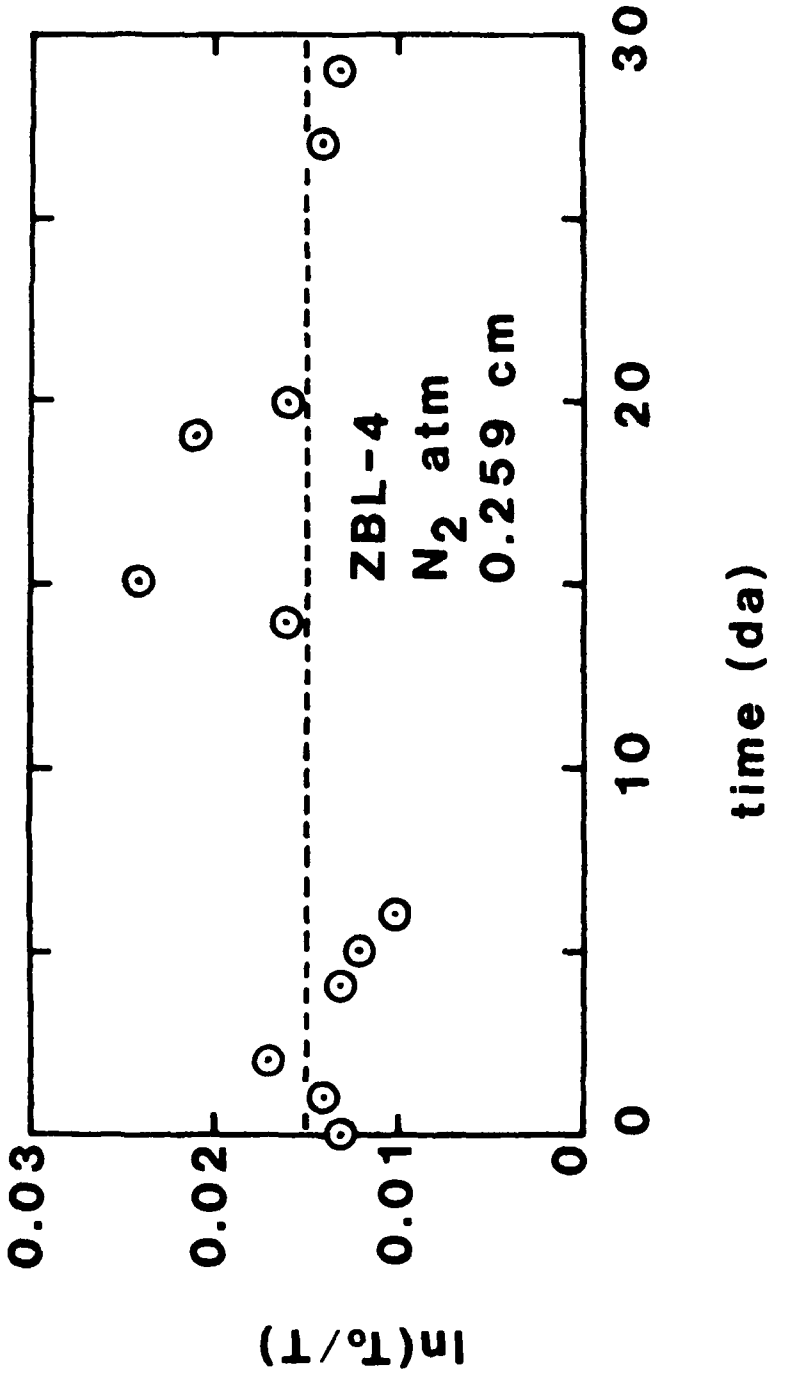
ln(T₀/T)
0.03
0.02
0.01
0
0
10
20
30
time (da)
ZBL-4
N2 atm
0.259 cm

previously reported[20,22] chemical inertness of these glasses in a neutral or basic aqueous environment.

Table IX shows the value of B in Eq. (1), i.e., the contribution to $\ln(T_o/T)$ at 3400 cm^{-1} from surface -OH, is of the order of 0.01 for the five glasses studied. This corresponds to a thickness independent loss in transmitted light intensity of about 1% at 3400 cm^{-1}, with correspondingly lower losses at frequencies removed from -OH band maximum. Losses of this magnitude are inconsequential for applications involving low to medium light intensities, e.g., fiber optic waveguides, but could become objectionable for high power applications, e.g., high energy laser windows.

References

1. M. G. Drexhage and P. K. Gupta "Strengthening of Glasses by Partial Leaching", J. Am. Ceram. Soc. 63 [1-2] 72(1980).

2. M. G. Drexhage "Strengthening of Glasses by Phase Separation" Ph. D. Dissertation, Catholic University of America, Washington, DC (1977).

3. D. A. Krohn and A. R. Cooper, "Strengthening of Glass Fibers: I" J. Am. Ceram. Soc. 52 [12] 661-64 (1976).

4. P. B. Macedo and T. A. Litovitz U. S. Patent 3,938,974 (1976).

5. J. H. Simmons, R. K. Mohr, D. C. Tran, P. B. Macedo and T. A. Litovitz, "Optical Properties of Waveguides Made by a Porous Glass Process" App. Optics 18 2732 (1979).

6. J. S. Stroud, J. Chem. Phys. , 35, 844 (1961).

7. H. S. Stroud, J. Chem. Phys. , 37, 836 (1962).

8. J. S. Stroud, Phys. Chem. Glasses, 5, 71 (1964).

9. A. M. Bishay, J. Am. Ceram. Soc. , 45, 389 (1962).

10. B. McGrath, H. Schunbacher and M. Van de Voorde, "Effects of Nuclear Radiation on the Optical Properties of Cerium-doped Glass" CERN 75-16, Geneva, 1975.

11. E. J. Friebele, Appl. Phys. Lett. , 27, 210 (1975).

12. A. Paul, M. Mulholland and M. S. Saman, J. Mater. Sci. , 11, 2082 (1976).

13. A. Barkatt, V. Ottolenghi and J. Rabbani, J. Phys. Chem. , 76, 203 (1972).

14. A. Barkatt, C. A. Angell and J. R. Miller, J. Am. Ceram. Soc. , 64, 158 (1981).

15. M. S. Matheson, Chapt. 10, "Reactions of Solvated Electrons," in Physical Chemistry Vol. VII, "Reactions in Condensed Phases", Academic Press, New York, New York 1975.

16. M. G. Drexhage, B. Bendow and C. T. Moynihan, "IR-transmitting Fluoride Glasses," Laser Focus, 16 [10] 62-68 (1980).

17. M. G. Drexhage, C. T. Moynihan, M. Saleh Boulos and K. P. Quinlan, "Fluoride Glasses for Visible to Mid-IR Guided Wave Optics,"Advances in Ceramics, Vol. II: Physics of Fiber Optics, American Ceramic Society, Inc. , Columbus, Ohio 1981.

18. M. G. Drexhage, C. T. Moynihan and M. Saleh, "Infrared Transmitting Glasses Based on Hafnium Flouride," Mat. Res. Bull. , 15 213-19 (1980).

19. A. Lecoq and M. Poulain, "Lanthanum Fluoride Glasses," J. Non-Cryst. Solids, 34 [1] 101-10 (1979).

20. M. Poulain and J. Lucas, "A New Class of Materials: Fluoride Glasses with Zirconium Tetrafluoride," Verres Refract. , 32 [4] 505-13 (1978).

21. S. Mitachi and T. Manabe, "Fluoride Glass Fiber for Infrared Transmision," Jap. J. Appl. Phys. , 19 [6] L313-14 (1980).

22. M. Robinson, R. C. Pastor, R. R. Turk, D. P. Devor and M. Braunstein, "Infrared Transparent Glasses Derived from the Fluorides of Zirconium, Thorium and Barium," Mat. Res. Bull. , 15 735-42 (1980).

MISSION
of
Rome Air Development Center

RADC plans and executes research, development, test and selected acquisition programs in support of Command, Control Communications and Intelligence (C^3I) activities. Technical and engineering support within areas of technical competence is provided to ESD Program Offices (POs) and other ESD elements. The principal technical mission areas are communications, electromagnetic guidance and control, surveillance of ground and aerospace objects, intelligence data collection and handling, information system technology, ionospheric propagation, solid state sciences, microwave physics and electronic reliability, maintainability and compatibility.

Printed by
United States Air Force
Hanscom AFB, Mass. 01731


DATE
FILMED
7-8